INTERNATIONAL JOURNAL OF CLIMATOLOGY
Int. J. Climatol. **18**: 299–316 (1998)

SPATIAL AND TEMPORAL PATTERNS OF ANNUAL PRECIPITATION VARIABILITY OVER THE IBERIAN PENINSULA

C. RODRIGUEZ-PUEBLA[a,*], A.H. ENCINAS[b], S. NIETO[b] and J. GARMENDIA[a]
[a] *Departmento Fisica de la Atmosfera, Universidad de Salamanca, Spain*
[b] *Departmento de Estadistica y Matematica Aplicadas, Universidad de Salamanca, Salamanca, Spain*

Received 26 November 1996
Revised 26 July 1997
Accepted 20 August 1997

ABSTRACT

In this study we have examined the spatial and temporal variability of the annual precipitation observations over the Iberian Peninsula (IP) for 47 years and 51 stations. Empirical orthogonal functions (EOFs) were obtained in order to characterise the variability. Four regional precipitation regimes have been identified and the corresponding principal components (PCs) were subjected to spectral analysis in order to obtain the structure of the temporal variations. The relationship between the precipitation and circulation patterns is also investigated. The four leading PCs of annual precipitation are associated with the following patterns: East Atlantic (EA); North Atlantic Oscillation (NAO); Southern Oscillation Index (SOI); Scandinavia (SCAND). The spectra of the precipitation PCs show statistically significant oscillations coherent with those found in the time series of the teleconnection indices. A reconstruction of the time series as a function of the PCs is provided in order to obtain a characterisation of precipitation climatology over the IP. © 1998 Royal Meteorological Society.

KEY WORDS: Iberia; Spanish climate; time series analysis; precipitation; teleconnections; principal component analysis; empirical orthogonal functions; spectral analysis

1. INTRODUCTION

Some of the problems that most interest the scientific community studying the atmosphere involve the description and analysis of climate variability. Rainfall is a major factor in agriculture and in recent years interest has increased in learning about precipitation variability and predictability for periods of months to years. We are concerned particularly about the threat of desertification throughout the Iberian Peninsula (hereafter IP). The precipitation time series appear to fluctuate randomly; however, a closer examination implies some regularity, and based on this behaviour we try to detect and estimate the interannual deterministic components or 'signals' within the observations in order to characterise some of the precipitation variations.

Krepper *et al.* (1989) have analysed monthly and seasonal rainfall in Argentina and determined the spatial and temporal variability using empirical orthogonal functions analysis; they also obtained the variance contribution of the spectral peaks. Recently, Rowell *et al.* (1995) used spectral analysis on the rainfall data in the north of Africa and obtained peaks at 3–8 years in Sudan and at 2–3 years in Guinea. Climatic fluctuations with several quasi-periods were found by Hogg (1995) in a study of time series of Canadian extreme rainfalls. Other authors have reported oscillations for different climate series: Vautard *et al.* (1992) applied singular spectral analysis (SSA) to global surface air temperature and found oscillations at 4.6, 5.2, 10, 7–8, 15 and 26 years; Labitzke and van Loon (1995) obtained the ten to twelve (TTO) year oscillation in the tropospheric temperature.

* Correspondence to: Departmento Fisica de la Atmosfera, Universidad de Salamanca; Spain. email: concha@gugu.usal.es

Contract grant sponsor: Ministry of Education and Science of Spain; Contract grant number: CICYT CLI96-1871-CO-04

CCC 0899–8418/98/030299–18$17.50
© 1998 Royal Meteorological Society

The origins of these variations are uncertain, although there are many studies that try to connect them with climate forcing factors such as solar activity, quasi-biennial oscillation (QBO) and oceanic and atmospheric circulation indices such as the El Niño–Southern Oscillation (ENSO). For example, Ropelewski and Halpert (1987), Vinnikov *et al*. (1990), Rasmusson and Arkin (1993), among others, have related the precipitation field in different parts of the globe to the ENSO phenomenon. Hastenrath and Greischar (1995) and Barnston and Smith (1996) proposed systems for precipitation prediction based on the empirical relationships between precipitation and atmospheric and oceanic indices.

The objectives of this paper are the following: to obtain the spatial patterns of precipitation variability; to determine interannual time-scales of precipitation variability; to explain some of the spatial patterns and temporal structures detected in the precipitation time series on the IP; to propose statistical models for the climate precipitation characterisation based on the regularities within the observations.

The paper is organised as follows: section 2 gives a description of the data set. The spatial patterns of precipitation variability and heterogeneous correlation patterns between teleconnection indices and precipitation are analysed in section 3; in section 4 the temporal structures are detected and a comparison between significant rainfall oscillations and those found in the indices is documented. The most significant conclusions are given in section 5. The methods used in this paper are referred to without explanation because they are well known and have often been described.

2. STATISTICS OF THE DATA BASE

Monthly rain-gauge data sets corresponding to 51 locations distributed irregularly throughout the IP, but with a fairly good uniform density (Figure 1), for the period 1949–1995 were the starting data to be analysed. The total monthly mean precipitation time series were provided by the National Meteorological

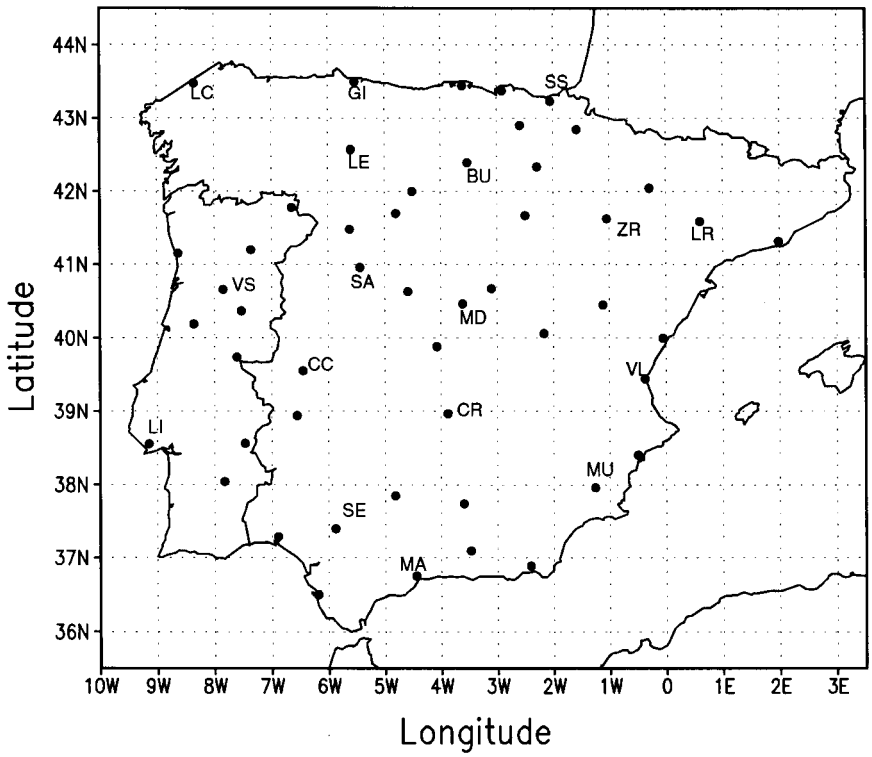

Figure 1. Map of the Iberian Peninsula with the stations used in this study. (See also Table I)

© 1998 Royal Meteorological Society

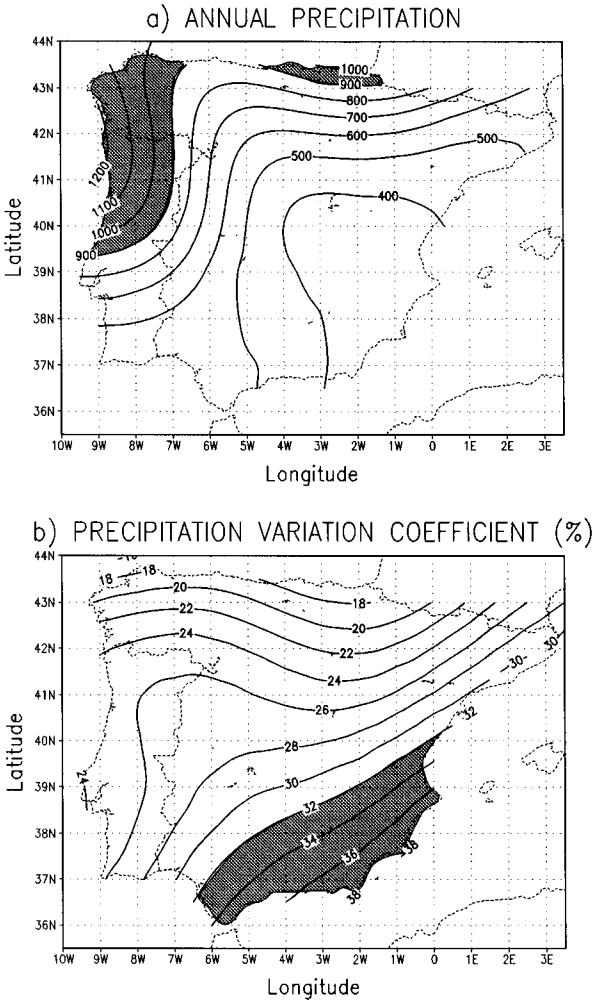

Figure 2. (a) Mean of the total annual precipitation over the Iberian peninsula for the period 1949–1995. (b) Percentage of variation coefficient over the Iberian peninsula for the period 1949–1995

Institutes of Spain and Portugal. When there were missing data in the time series we proceeded in the following way: first, the corresponding monthly mean substituted the missing values; second, the correlation matrix was computed among the time series, in order to select the four surrounding precipitation time series with rainfall characteristics that most closely resembled those of the station with missing data; a linear spatial regression was then derived to interpolate the missing values, the method being similar to the one proposed by Peterson and Easterling (1994) to create reference time series for testing inhomogeneities. Time series of annual accumulated rainfall were estimated for this study.

Figure 2(a) shows the precipitation climatology (mean of the total annual precipitation for the period 1949–1995) over the IP. The distribution of precipitation reveals strong gradients, with higher values corresponding to the west and the north of the IP (> 1000 mm year^{-1}) and lower values obtained toward the southeast of the IP (< 400 mm year^{-1}). There are also inland regions with a relatively low precipitation regime. The pattern of the precipitation variation coefficients (defined by the percentage of the standard deviation divided by mean) is shown in Figure 2(b); the higher values were obtained towards the southeast of the IP.

Table I depicts the statistics of the annual rainfall time series for 17 selected stations shown in Figure 1. The columns depict the elevation (EL), the mean annual rainfall in mm year^{-1} (RM), the standard

© 1998 Royal Meteorological Society

deviation in mm year^{-1} (SD), the skewness (SK) or measure of the symmetry of the distribution, and the kurtosis (KT) or peakedness of the distribution. Most of the time series can be considered as mesokurtic because the kurtosis results fall between the corresponding critical values (-0.97 and 1.4) (Ardanuy and Soldevilla, 1992), however, the time series are positively skewed, which means that the larger rainfall values are less frequent and the data follow a gamma distribution, which should be considered when reporting precipitation prediction probabilities (Briggs and Wilks, 1996).

Figure 3 shows the monthly mean annual evolution of the precipitation for 17 selected locations and for two periods: (a) 1949–1995 (solid line); (b) 1986–1995 (dashed line). The percentages of seasonal precipitation compared with annual precipitation are: 33% for Winter (December, January and February), 26% for spring (March, April and May), 12% for summer (June, July and August) and 29% for autumn (September, October and November). The main characteristic is the scarcity of summer rains. In the north and the west of the IP the highest rainfall regime was obtained in winter, in the south and east of the IP the highest rainfall was obtained in autumn, and different behaviour was found in the centre of the IP, with higher precipitation in either spring or autumn, which is in accordance with previous studies by Font Tullot (1983, 1988).

The reason for comparing the annual evolution of the precipitation in most recent years with the longer period is to provide some information on the different tendency according to the seasons. In most stations a precipitation decrease is observed in the period 1986–1995 compared with the period 1949–1995 for the winter season, which is in agreement with the $2 \times CO_2$ simulation experiment of Von Storch *et al.* (1993); however, some stations show an increase in precipitation for autumn and spring during the last decade compared with the entire period. An attempt to find an explanation for the different tendency is given in section four by comparison with the tendency of the rainfall principal components and the teleconnection circulation indices associated with the annual precipitation.

Persistence, trend and periodic fluctuations are the common forms of non-random variations in the climate. Discovery of their statistical significance is the first step toward the physical explanation of climate variations. Serial correlation at lag -1, the Mann–Kendall test and spectral analysis were the statistical tools used to obtain the significance of the variations. Table I depicts the results of persistence and trend testing for 17 selected locations. The autocorrelations at lag -1 (r_1) do not show evidence of a significant persistence, with exceptions in MA and SE. According to the results obtained with the

Table I. Statistics of the annual rainfall time series for 17 stations. EL, elevation; RM, annual mean precipitation; SD, standard deviation; SK, skewness; KT, kurtosis; r_1, autocorrelation coefficient; τ, Mann–Kendall statistics test

Station	EL (m)	RM (mm year^{-1})	SD	SK	KT	r_1	τ
BU (Burgos)	881	569	144	0.35	1.1	0.17	0.11
CC (Caceres)	459	493	134	0.43	−0.67	−0.07	0.08
CR (CiudadReal)	629	426	131	0.94	1.14	0.15	−0.17
GI (Gijon)	10	961	135	0.31	−0.17	0.05	−0.03
LC (La Coruña)	67	996	168	0.54	−0.37	0.18	−0.01
LE (Leon)	913	554	129	0.34	−0.69	0.09	−0.07
LR (Lerida)	202	358	94	0.50	−0.53	−0.09	−0.14
LI (Lisbon)	77	736	191	0.62	0.33	0.05	−0.07
MA (Malaga)	7	546	214	1.24	1.45	0.25	−0.14
MD (Madrid)	667	443	120	0.53	−0.18	−0.02	−0.15
MU (Murcia)	75	296	111	0.41	−0.28	−0.04	−0.03
SA (Salamanca)	790	384	95	0.68	−0.30	0.12	−0.04
SE (Sevilla)	31	572	192	0.68	−0.24	0.22	−0.13
SS (San Sebastian)	259	1560	224	0.06	0.29	0.09	−0.03
VL (Valencia)	11	451	172	1.00	1.10	−0.08	−0.01
VS (Viseu)	600	1120	336	0.43	−0.59	0.06	−0.08
ZR (Zaragoza)	240	321	86	1.22	2.70	−0.06	−0.19

© 1998 Royal Meteorological Society

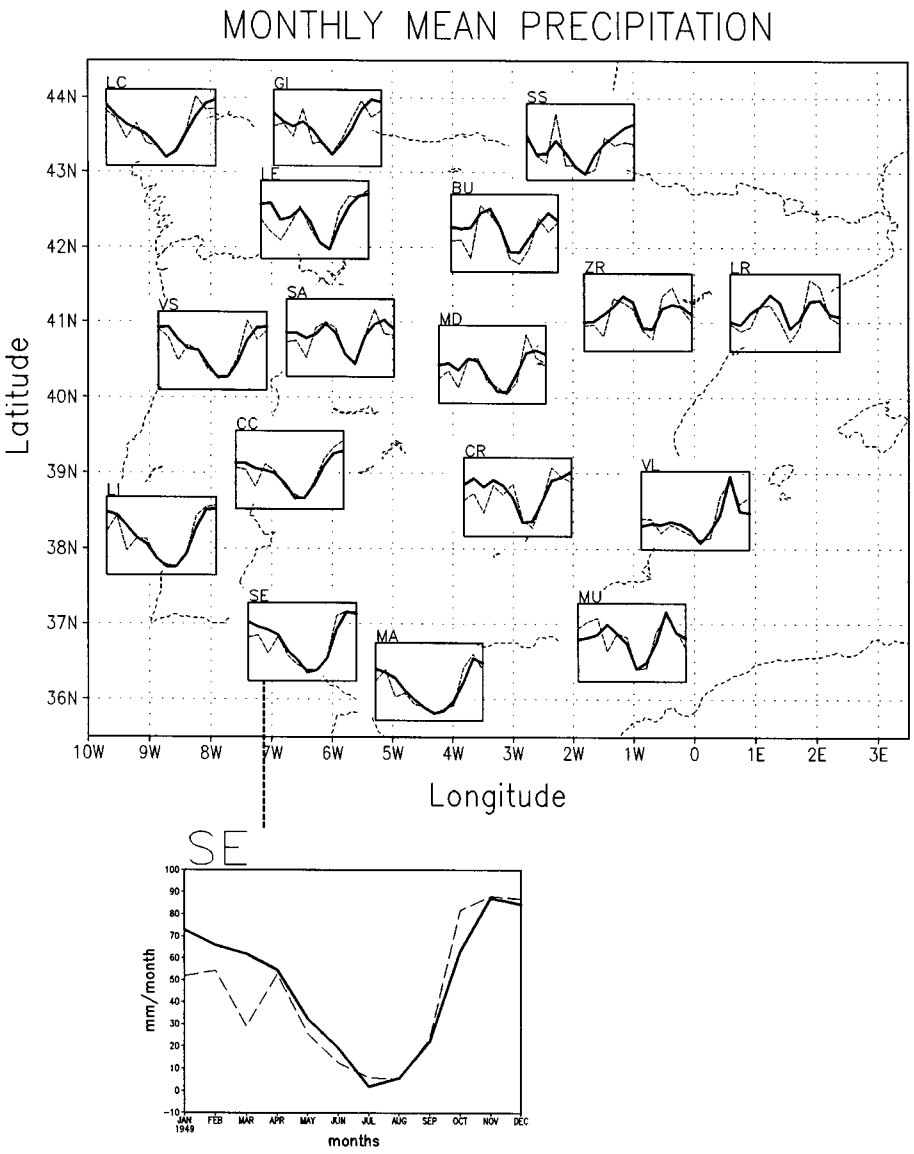

Figure 3. Monthly mean annual evolution of precipitation for 17 stations and two periods. Solid line, 1949–1995; dashed line, 1986–1995

Mann–Kendall statistic (τ) (Mitchell *et al.*, 1966; Sneyers, 1990), the majority of the time series provided negative values (Table I). Although MA and SE have a significant τ value, these results must be due to their serial correlation (Kulkarni and von Storch, 1995); however, MD and ZR exhibit a decreasing trend with no significant persistence. In Figure 4 the Kendall τ coefficient is shown to consider the slight tendency towards lower precipitation regime over some regions of the peninsula, with larger values towards the south. Hulme (1995) examined zonal changes in precipitation and obtained a strong contrast between tropical latitudes (drying) and the high latitudes (wetting).

The precipitation time series are quite irregular (Rodriguez *et al.*, 1992); on the other hand, the spectra obtained (not shown) are broadband with energy at many frequencies and dissimilarities even among neighbouring locations, due, in certain aspects, to errors in measurement. The spectra of different realizations of longer precipitation time series (approximately 100 years) were compared and the results

© 1998 Royal Meteorological Society

indicate that the spectra are not temporally stable. Therefore, it would not be possible to detect stable signals from the local precipitation series. However, spatial averaging reduces the noise component and increases the signals. In order to average the time series they must have approximately the same statistical structure. For that reason, we have used principal component analysis, in *S*-mode (Preisendorfer, 1988), to reveal spatial regions where observations have similar statistical structure and, thus, averaging is permissible. Varimax orthogonal rotation is the option used to avoid some of the domain shape dependence (Richman, 1986) and to obtain stable and physically meaningful patterns (Von Storch, 1995). The space variance of precipitation distribution is given by the eigenvector maps or EOFs. The eigenvalues of EOFs indicate the amount of variance accounted for by a pattern. The projection of the time series observations on to the eigenvectors are called principal components (hereafter PCs); these were subjected to spectral analysis in order to determine the time-scale variability.

3. SPATIAL VARIABILITY

The rotated empirical orthogonal functions (EOFs) obtained from the total annual standardised precipitation data set (anomaly divided by standard deviation) allow us to recognise the regions with different precipitation climatology; they are also used to filter out some errors in the precipitation observations and to reconstruct the precipitation time series depending on the significant principal components.

Figure 5 shows the spectrum of eigenvalues and the noise spectrum given by an analytical formula (Cahalan, 1983), in order to distinguish 'signal' from 'noise'. From the comparison of the lines only the four leading EOFs were above the noise and they could represent physical inhomogeneities. The leading EOF accounts for 33% of total variance, the second leading EOF accounts for 19%, and the third and fourth account for 14% and 13%, respectively.

The sampling errors of the EOFs estimated (North *et al.*, 1982) are shown by the error bar in Figure 5; degeneracy occurs when the difference between nearby eigenvalues is less than the sampling error. There is overlapping among the error bars of the modes, and the patterns are mixed; as a result some uncertainties in obtaining the meaning for the patterns are unavoidable.

The inhomogeneities in the precipitation time series must be due to physical causes and are connected, in general, with anomalies in the large-scale general circulation of the atmosphere; therefore, we have considered the teleconnection indices proposed by Barnston and Livezey (1987) to analyse the precipitation fluctuations. The indices are centres of action of anomalies in the mid- to upper tropospheric geopotential field. Leathers *et al.* (1991) obtained correlation between the Pacific North America

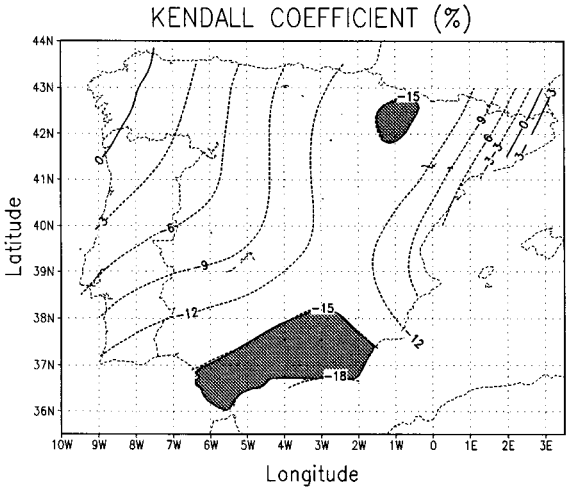

Figure 4. Kendall coefficient pattern for the period 1949–1995

© 1998 Royal Meteorological Society

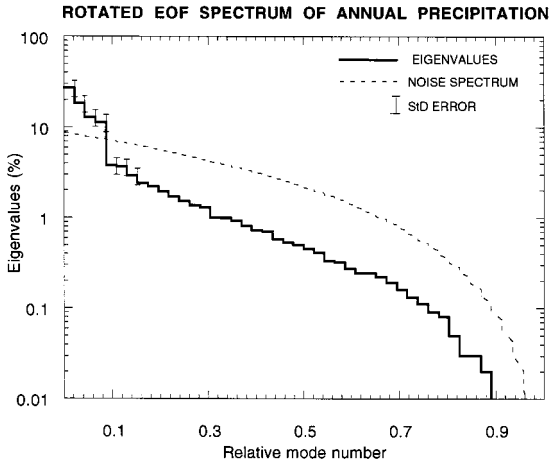

Figure 5. Spectrum of empirical orthogonal functions. The dashed curve is the analytic noise spectrum. The staircase is the percentage of the variance associated with each eigenvalue. The error bar is standard error for the first five eigenvalues

teleconnection index (PNA) with temperature and precipitation in the USA and propose the teleconnection indices as a resource in the discussion of climate change and variation. Circulation indices were used by Drosdowsky (1993) to explain Australian rainfall; Corte Real *et al.* (1995) related the large-scale sea-level pressure to monthly rainfall in Portugal; and Kutiel *et al.* (1996) also examined the changes of summer precipitation in the eastern Mediterranean and the variations in surface circulation indices.

The pattern of the rotated EOF1 (Figure 6(a)) exhibits positive values over the whole of the IP, with higher values towards the western regions. The corresponding principal component (PC1) is significantly correlated with the April East Atlantic (EA) teleconnection index ($r = 0.39$). The EA pattern consists of a north–south dipole that spans the entire North Atlantic Ocean with the centres near 55°N, 20–35°W and 25–35°N, 0–10°W. Figure 6(b) shows the heterogeneous correlation map between the teleconnection index and the total annual precipitation over the IP. The shapes of the contour lines of Figure 6(a) and 6(b) are quite similar. The coupled signal of EA and precipitation is similar to the leading EOF of the precipitation field. The weather regime associated with the EA contains a strong subtropical link and it is responsible for the first mode of precipitation variability over the IP.

The second rotated EOF explains 19% of total precipitation variance; higher values were obtained toward the south-western part of the Iberian peninsula and lower values were obtained in the north of the peninsula (Figure 7(a)).

The North Atlantic Oscillation (NAO) index identified by Wallace and Gutzler (1981) consists of a north–south dipole of geopotential anomalies, with one centre located over Greenland and the other spanning between 35°N and 40°N in the central North Atlantic. The NAO teleconnection index obtained by Barnston and Livezey (1987) is used to obtain meanings of the second mode of precipitation variability. The results of the correlation between precipitation and NAO indices indicate that the December NAO is significantly correlated with the second principal component of annual precipitation variability (PC2), the correlation coefficient being equal to -0.42. Figure 7(b) shows the heterogeneous correlation map between the NAO teleconnection index and annual precipitation over the IP, and the shapes of Figure 7(a) and 7(b) have a similar distribution. The results indicate the coupling between NAO and Iberian precipitation. This conclusion was expected according to previous results obtained by Lamb and Pepler (1987), who demonstrated the significance of NAO for the long-range prediction of Moroccan winter precipitation.

The third eigenvector of the precipitation field (Figure 8(a)) corresponds to an eigenvalue of 14%; it divides the Iberian peninsula into west–east precipitation regimes, with higher values towards the east and lower values towards the northwest. No significant correlations have been found between Northern Hemisphere teleconnection indices and PC3.

© 1998 Royal Meteorological Society

Trying to find connections between precipitation over the IP and Southern Oscillation Index (SOI), Rodo *et al.* (1997) have identified the significant influence of El Niño–Southern Oscillation (ENSO) for spring and autumn precipitation in the eastern part of Spain. Moreover, Peixoto and Oort (1992) stated that one of the most important aspects of ENSO is the change in precipitation patterns over the globe. Fraedrich and Muller (1992) investigated the response of the Atlantic storm track during warm and cold events and found some evidence of the influence of ENSO on surface pressure, temperature and precipitation over Europe. Ropelewski and Halpert (1987) found regions in northern Africa and southern Europe with an apparent ENSO precipitation relationship. Further studies of Kiladis and Diaz (1989) obtained wetter than normal conditions in the western Mediterranean during a cold event; Rasmusson and Arkin (1993) also documented the outgoing longwave radiation (OLR) anomalies and Atlantic–African cloud-band variations during the 1982–1983 warm episode. These considerations motivate us to analyse the effects of SOI (standardised differences in sea-level pressure between Tahiti and Darwin) on the annual precipitation over the IP. The results obtained demonstrate that the third principal component of total annual precipitation is significantly correlated with the October SOI of the previous year ($r = 0.58$). The heterogeneous correlation map between the October SOI index and the following year's precipitation over the peninsula (Figure 8(b)) shows the areas under the SOI influence; this result is in agreement with the study of Rodo *et al.* (1997).

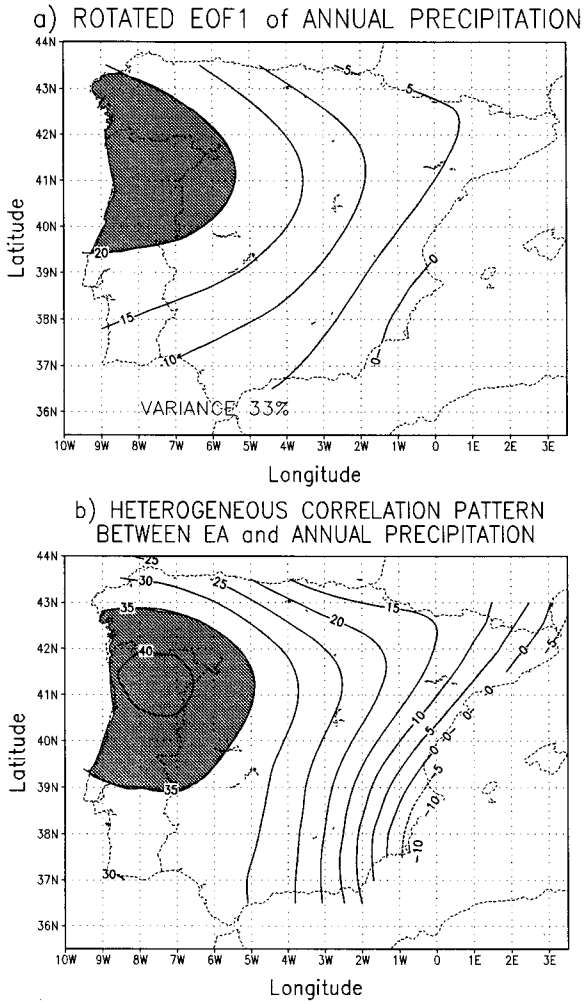

Figure 6. (a) First rotated EOF of annual precipitation. (b) Heterogeneous correlation pattern between the April East Atlantic pattern and annual precipitation

© 1998 Royal Meteorological Society

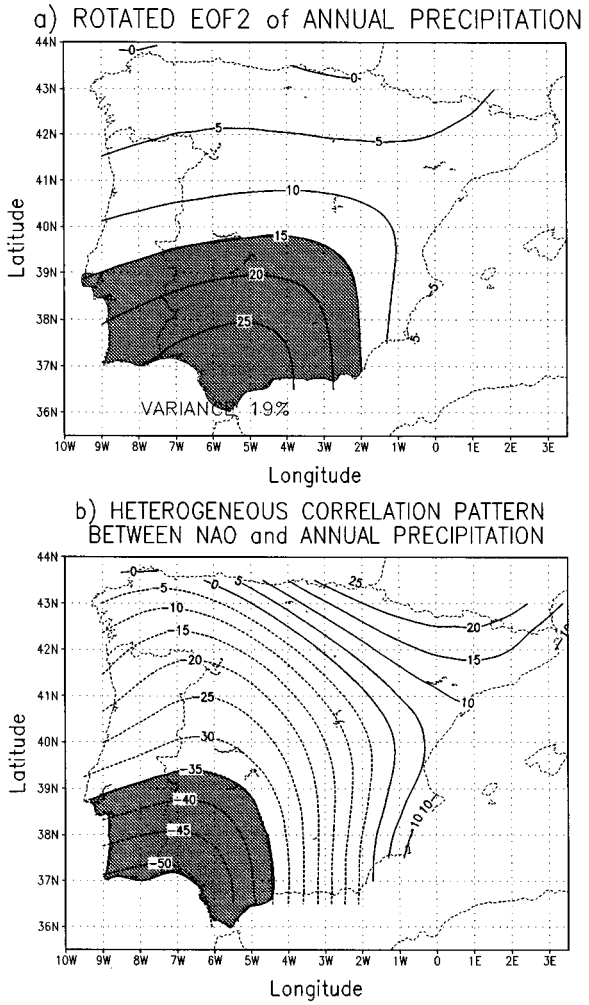

Figure 7. (a) Second rotated EOF of annual precipitation. (b) Heterogeneous correlation pattern between the December North Atlantic Oscillation and annual precipitation

The fourth rotated EOF explains 13% of total variance; Figure 9(a) shows the spatial distribution, with higher values in the northern part of the peninsula. Significant correlation was found between the corresponding principal component (PC4) of annual precipitation and the December Scandinavia (SCAND) pattern ($r = 0.36$). The SCAND pattern consists of a circulation centre that spans Scandinavia and large portions of the Arctic Ocean. One additional centre with the opposite sign is located over western Europe. This pattern is referred to as the Eurasia-1 pattern by Barnston and Livezey (1987). Figure 9(b) shows the heterogeneous correlation map between the SCAND index and the annual precipitation; some of the annual precipitation variability in the northern part of Spain is related to the SCAND December pattern.

The major atmospheric influence on annual IP precipitation variability is due to the EA, NAO, SOI and SCAND teleconnection indices. The relationships between rainfall and either atmospheric and oceanic indices can be used for down-scaling (Zorita *et al.*, 1992, 1995) and long-range precipitation predictions (Barnston and Smith, 1996).

Further topographic factors must be considered to characterise the background precipitation climatology. Egido *et al.* (1991) analysed the precipitation over the Spanish Tagus river basin as a function of

© 1998 Royal Meteorological Society

Table II. Correlation coefficients between EOFs of the precipitation field and geotopographic factors

Geofactors	EOF1	EOF2	EOF3	EOF4
Latitude	0.15	0.79	−0.30	0.73
Longitude	−0.71	−0.28	0.63	0.31
Elevation	0.46	−0.07	−0.00	0.06

topographic factors and a greater influence of elevation was obtained. Table II depicts the correlation between the annual patterns of precipitation variability and elevation, latitude and longitude. The dependency of precipitation on elevation is given by EOF1; the other patterns include most of the synoptic influences.

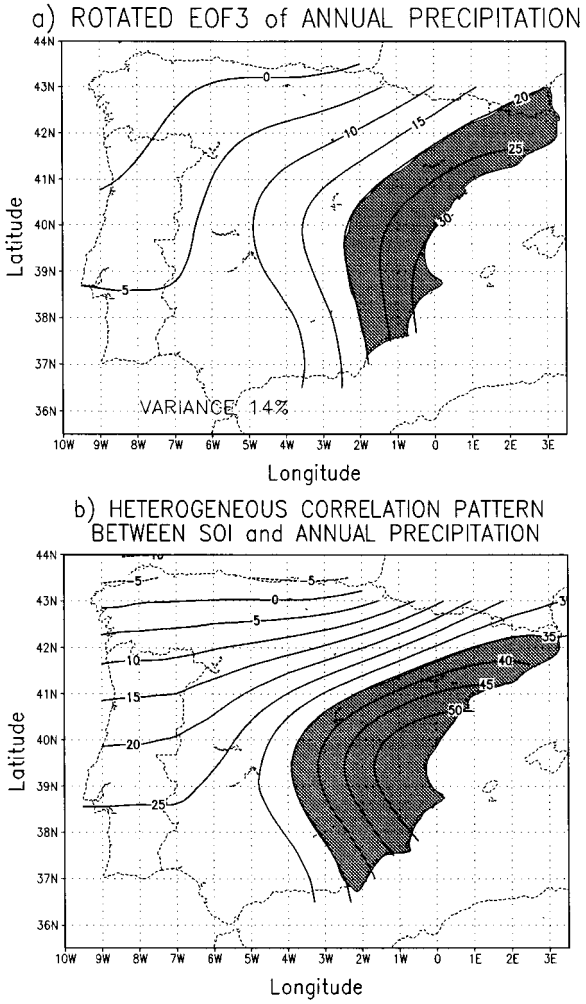

Figure 8. (a) Third rotated EOF of annual precipitation. (b) Heterogeneous correlation pattern between the October of the previous year's Southern Oscillation Index and annual precipitation

© 1998 Royal Meteorological Society

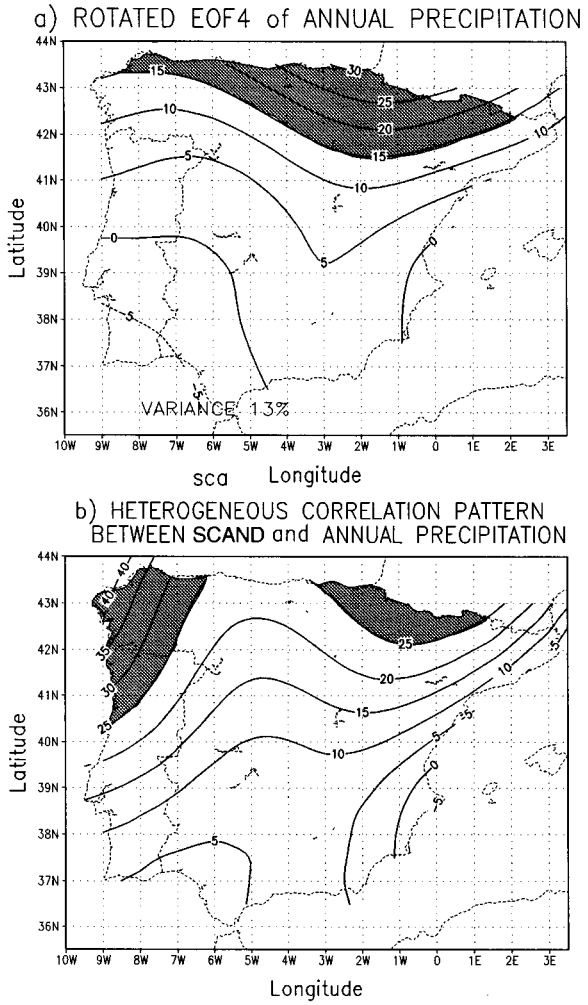

Figure 9. (a) Fourth rotated EOF of annual precipitation. (b) Heterogeneous correlation pattern between the December Scandinavia pattern and annual precipitation

4. TIME-SCALE VARIABILITY

The time-scale variability was obtained using spectral analysis on the principal components (PCs) of rainfall. Time series consist of an infinite number of oscillations and the spectral analysis, with the stationary assumption, distributes the variance from the lowest to the Nyquist frequencies (Chatfield, 1980). We have used the Blackman and Tukey procedure to compute the spectrum, which is based on the Fourier transform of the serial correlation coefficients and smoothed with an appropriate bandwidth to derive a consistent estimate of the spectrum (Brockwell and Davis, 1987; Dixon *et al.*, 1988). The Markov red noise spectrum (Mitchell *et al.*, 1966) has been considered as a test of statistical significance of the peaks.

The spectrum of the first principal component (PC1) exhibits a broad peak spanning the range of 4 and 6 years (Figure 10(a)). The peaks exceed the red noise spectrum but not the 95% significance level. The spectrum of the EA teleconnection index (Figure 10(b)) shows peaks at 4–5 years with significance at the 95% level. The 5-year period oscillations of PC1 and EA have a coherency squared of 0.72.

The spectrum of the second principal component (PC2) of precipitation (Figure 10(c)) shows a pronounced peak at 7–9 years. The spectrum of the NAO index (Figure 10(d)) shows the peaks at 7–9

© 1998 Royal Meteorological Society

years, which are coherent (Figure 10(c)) with the oscillations of PC2; the coherency squared is 0.87. Hurrell and van Loon (1995) also obtained the spectrum of the NAO index with enhanced variance at 6–10 year periods, and they suggest a strong relationship between the NAO index and temperature over northern Europe due to the similarities between the NAO and Copenhagen temperature spectra. The presence of the 7–9 year peaks in both series, as well as in previous results about the correlation map between the NAO index and precipitation time series, confirm the importance of considering the NAO index in explaining precipitation variability over the IP.

The spectrum of PC3 (Figure 10(e)) shows a significant oscillation for 16 years and a broad peak for 2 and 3 years. The SOI index also has peaks for 16, 5, 3 and 2.4 years (Figure 10(f)). The 16-year-period oscillations have a coherency squared of 0.82.

The spectra of PC4 (Figure 10(g)) and the SCAND index (Figure 10(h)) have significant oscillations at 6.5 years, which have a coherence of about 0.69.

The most significant oscillations of the rainfall PCs were filtered by means of fitting the data to four harmonic functions and estimating the amplitude and phase using the Levenberg–Marquardt algorithm or non-linear least-squares routine (IMSL, 1991). The residual time series was fitted to an autoregressive model (order one or two) and found to be significant (Chatfield, 1980). A linear regression model depending on the oscillations and autoregressive component was proposed to compute the PCs; the explained variances of the predictors are in Table III. The most important oscillations are: 3–6 years for PC1; 6–9 years for PC2; 16 years and 2–3 years for PC3; 6–9 years for PC4.

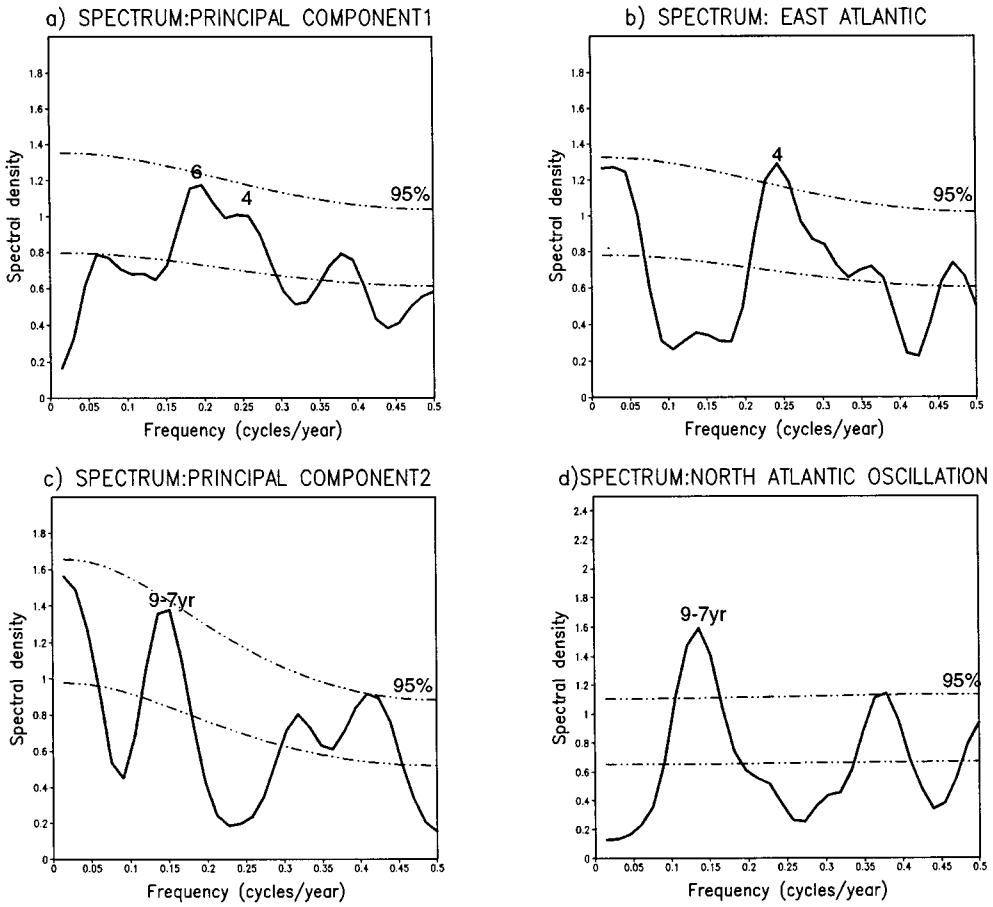

Figure 10. (a), (c), (e) and (g) are the spectra of the four leading PCs of annual precipitation (solid line); the dot-dashed lines are the Markov red noise spectrum and the 95% level of significance. (b), (d), (f) and (h) are the spectra of the EA, NAO, SOI and SCAND teleconnection patterns

© 1998 Royal Meteorological Society

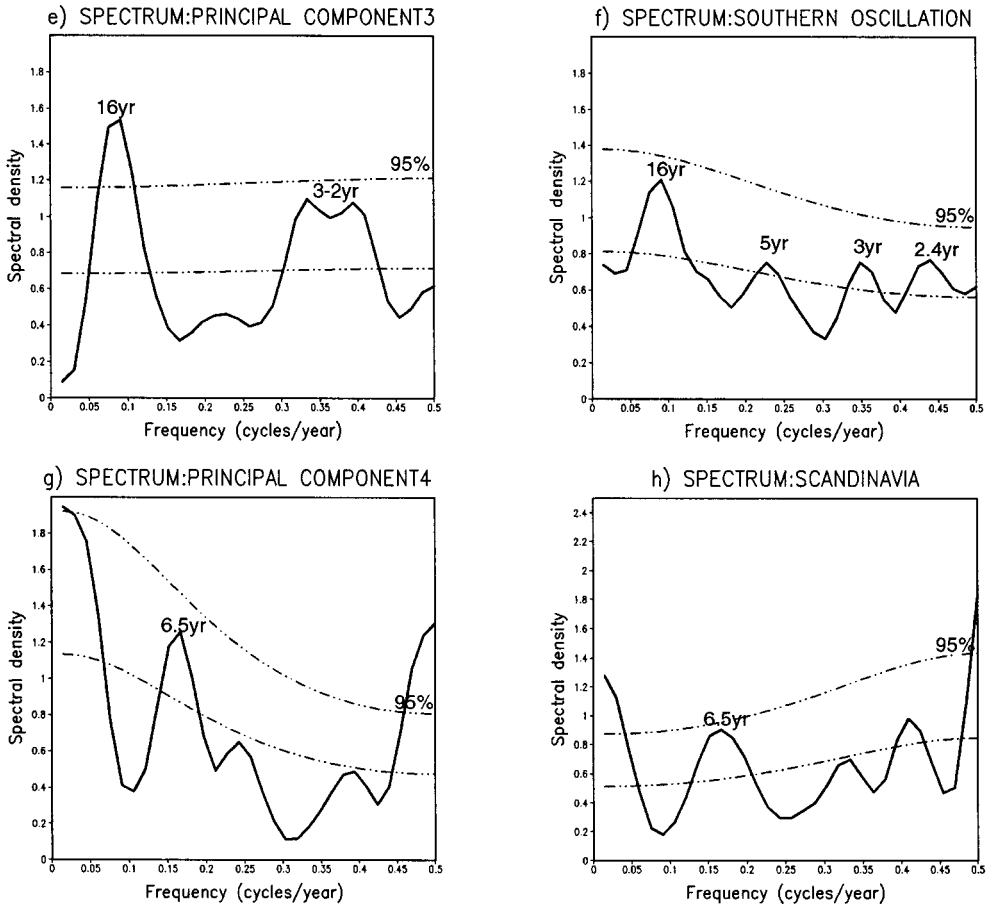

Figure 10 (*Continued*)

Time series of the principal components and the teleconnection indices are presented in Figure 11.

(i) The higher value of PC1 (Figure 11(a)) corresponds to the year 1959; in October 1959 a deep low pressure travelled through the peninsula and heavy rainfall and flooding occurred at stations in Portugal and Castilla–Leon, with rainfall approximately 50% higher than normal. The highest value for the EA index also corresponds to the year 1959 (Figure 11(b)).

(ii) The decreasing trend observed in PC2 (Kendall coefficient = -0.23) expresses the precipitation decrease in winter. One singular year was 1963, with the highest value for PC2 (Figure 11(c)) and a low NAO index (Figure 11(d)); during December 1963 heavy precipitation occurred toward the southern part of the peninsula.

Table III. Percentage of variance explained by the significant oscillations and the autorregressive function (AR) of the principal components of annual rainfall

EOFs	Period in years						
	2–3	3.1–6	6.1–9	*ca.* 9.1–12	*ca.* 16	≥20	AR
EOF1		24				11	13
EOF2	10	6	19			15	
EOF3	20			10	22		5
EOF4	14	6	20			20	

© 1998 Royal Meteorological Society

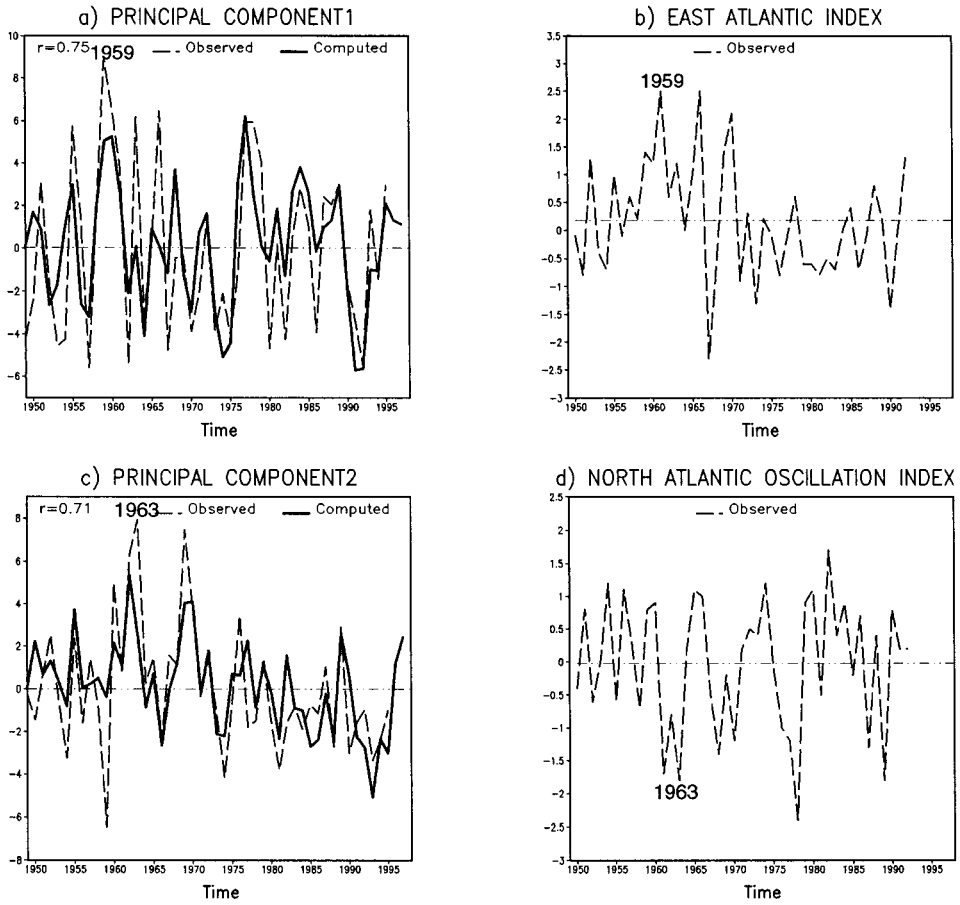

Figure 11. (a), (c), (e) and (g) are the time series of the four principal components: the dashed lines are from the observational data set, the solid lines are the PCs computed from the models. (b), (d), (f) and (h) are the time series of the EA, NAO, SOI and SCAND teleconnection indices

(iii) Wheeler and Tout (1990) have discussed the autumn rainfall regime on the Spanish Mediterranean coast for 1989; in this singular year heavy rainfall occurred in October towards the Mediterranean coast and also heavy rainfall was received in the south-western part of the peninsula in December; however, it was one of the driest years in the northern part of the peninsula. In Figure 11(e) and 11(g) it can be observed that PC3 has the highest value, but PC4 has the lowest value. Furthermore the SCAND index has a negative value for the year 1989. Two important circumstances have to be mentioned relating to the year 1989. On one hand, the NAO index was negative, which caused heavy rainfall in the south. On the other hand, in 1988 a cold event developed which corresponded to a positive SOI (Figure 11(f)). A positive correlation between the October SOI and the following year precipitation was obtained, the higher correlation coefficients being towards eastern Spain. Therefore, the 1988 cold event could have affected the rainfall over the Mediterranean region. The SCAND index shows a decreasing trend (Kendall coefficient $= -0.26$) that could be related to the decreasing winter precipitation.

When spectral analysis was applied to the local precipitation time series, multiple temporal scales were obtained with relatively significant variance and it is therefore difficult to identify spatially organised structures in the spectra. One possible solution, in order to obtain a rational temporal decomposition, is to create less contaminated time series and to reconstruct the precipitation time series by removing the noise. We have considered the four significant rotated EOFs and we have used linear stepwise regression

© 1998 Royal Meteorological Society

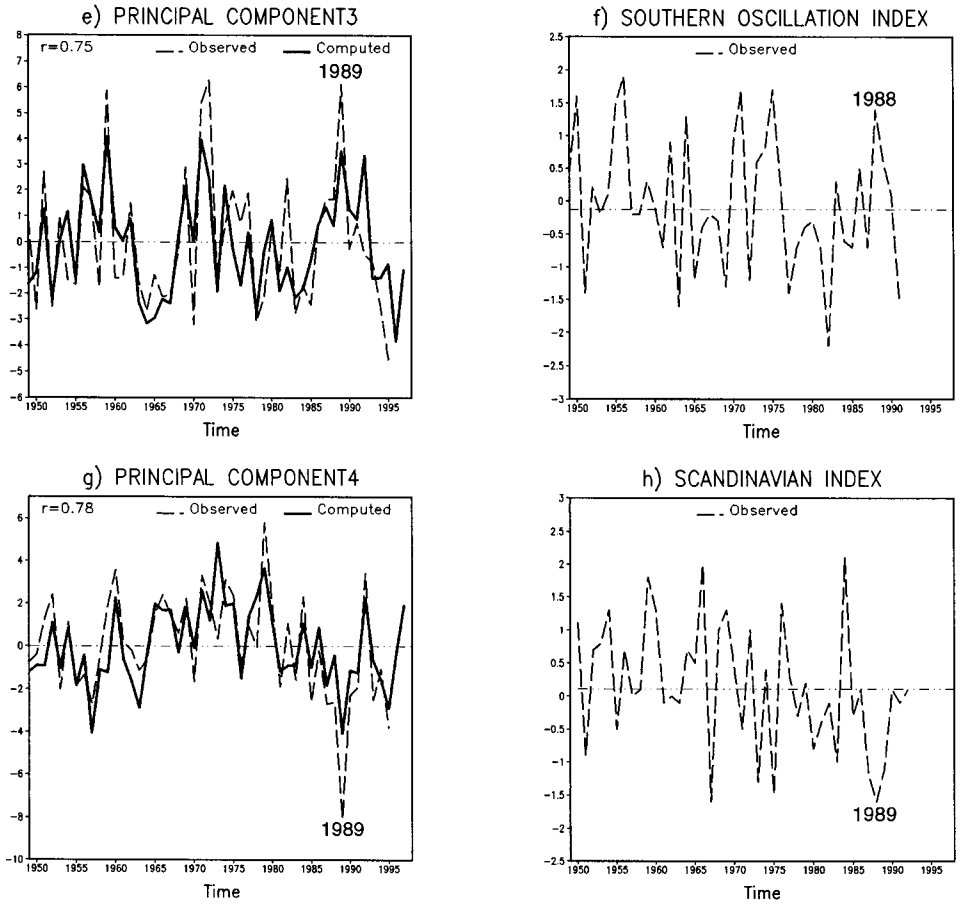

Figure 11 (*Continued*)

to select the EOF predictors associated with the local precipitation. Table IV depicts the regression coefficients, the constant and the correlation of the linear models obtained to reconstruct the precipitation time series for 17 selected locations. Some models consider four PCs and others consider three, two or one; the results are consistent with the precipitation regionalisation given by EOFs.

One of the applications of our investigation is to provide sources of long-range precipitation outcomes in local stations through building models from available data. The models are based on the reconstruction of the significant 'signals' from the space and time data. The proposed models consider the interannual variability and therefore have some advantage with respect to the climate normals or the mean of recent years (Huang *et al.*, 1996; Briggs and Wilks 1996; Wilks, 1996).

5. CONCLUSIONS

In order to detect climate change it is necessary to have determined the space–time distribution of the natural variability. In this study we have documented information on the spatial and temporal structures of annual precipitation over the Iberian Peninsula. Spectral analysis, empirical orthogonal functions and multiple regression methods were used to examine the modes of variation. The following conclusions were obtained.

The leading rotated empirical orthogonal function of annual precipitation accounts for 33% of the total variance; it represents precipitation variability over western regions of the peninsula and is associated with

© 1998 Royal Meteorological Society

Table IV. Regression, constant, and correlation coefficients of the linear models that reconstruct the precipitation time series from the significant principal components, for 17 stations

Station	EOF1	EOF2	EOF3	EOF4	Constant	*r*
BU (Burgos)	24.8	14.0		25.9	569	0.85
CC (Caceres)	26.2	19.3		−5.9	493	0.89
CR (CiudadReal)	11.4	33.8	13.1	12.3	427	0.90
GI (Gijon)				41.4	961	0.74
LC (La Coruña)	31.8			27.2	996	0.84
LE (Leon)	27.5		10.8		554	0.86
LR (Lerida)		6.2	19.3	19.4	358	0.76
LI (Lisbon)	34.6	34.8		−11.9	736	0.90
MA (Malaga)		51.5	31.5		546	0.80
MD (Madrid)	18.8	18.2	21.1		444	0.89
MU (Murcia)			33.8		296	0.78
SA (Salamanca)	19.9	7.6	6.6		384	0.87
SE (Sevilla)	17.3	54.8	10.5	−11.7	572	0.93
SS (San Sebastian)			−21.8	66.0	1560	0.76
VL (Valencia)		12.3	50.9		452	0.79
VS (Viseu)	75.2	28.4			1199	0.91
ZR (Zaragoza)	5.3		23.7	10.7	321	0.81

the April East Atlantic teleconnection pattern defined by Barnston and Livezey (1987). The second empirical orthogonal function explains 19% of total precipitation variance, with higher values towards the south-western part of the peninsula and it is associated with the December North Atlantic Oscillation pattern. The third empirical orthogonal function explains 14% of total variance, with higher values towards the east; it is associated with the October Southern Oscillation Index of the previous year. The fourth rotated EOF explains 13% of total variance and it is associated with the Scandinavia teleconnection pattern.

The most significant oscillations are: 3–6 years for PC1; 6–9 years for PC2; 16 years and 2–3 years for PC3; 6–9 years for PC4. The oscillations are coherent with those found in the teleconnection indices.

The singular years of 1959, 1963 and 1989 are discussed by comparison of the time series of the principal components and the teleconnection circulation indices.

One of the applications of our investigation is the possibility of providing sources of long-range precipitation outcomes in local stations through building models from available data. The models are based on the reconstruction of the significant 'signals' from the space and time data.

We are aware that precipitation is a chaotic process, and that predictions need hybridisation of different models. In spite of this, the simple simulation of the behaviour, of the system may give guidance for planning and obtaining a predictability of drought and flood events. We will continue analysing seasonal and monthly precipitation time series and examining how regional precipitation is affected by atmospheric circulations and the ocean in order to understand the physics responsible for the rainfall variations and to derive empirical models.

ACKNOWLEDGEMENTS

The authors would like to thank the anonymous reviewers for their helpful comments. We are also grateful to Dr R.F. Cahalan for valuable recommendations on the EOF spectrum significance, E. Zorita, H. Kutiel and E. Foufoula-Georgiou for their fruitful suggestions. We wish to thank the National Institute of Meteorology of Spain and Portugal for providing the data and D. Garvey for the English review. This paper is supported by Ministry of Education and Science under project CICYT CLI96-1871-CO-04. GrADS software was used for drawing the graphics.

© 1998 Royal Meteorological Society

REFERENCES

Ardanuy, R. and Soldevilla, M.M. 1992. *Estadistica Basica*, Hesperides.

Barnston, A. and Smith, T.M. 1996. 'Specification and prediction of global surface temperature and precipitation from global SST using CCA', *J. Climate*, **9**, 2660–2697.

Barnston, A.G. and Livezey, R.E. 1987. 'Classification, seasonality and persistence of low-frequency atmospheric circulation patterns', *Mon. Wea. Rev.*, **115**, 1083–1126.

Briggs, W.M. and Wilks, D.S. 1996. 'Estimating monthly and seasonal distributions of temperature and precipitation using the new CPC long-range forecasts', *J. Climate*, **9**, 818–839.

Brockwell, P.J. and Davis, R.A 1987. *Time Series: Theory and Methods*, Springer-Verlag, Berlin, pp. 320–386

Cahalan, R.F. 1983. 'EOF spectral estimation in climate analysis', *Proceedings of the Second International Meeting on Statistical Climatology*, *Lisbon*, *Portugal*, 4.5.1–4.5.7.

Chatfield, C. 1980. *The analysis of time series. An introduction*, Chapman and Hall, London

Corte Real, J., Zhang, X. and Wang, X. 1995. 'Large-scale circulation regimes and surface climatic anomalies over the Mediterranean', *Int. J. Climatol.*, **15**, 1135–1150.

Dixon, W.J., Brown, M.B., Engelman, L. and Jennrich, R.I. 1988. *BMDP Statistical Software Manual*, Vols 1 and 2, UCLA.

Drosdowsky, W. 1993. 'An analysis of Australian seasonal rainfall anomalies: 1950–1987. II: Temporal variability and teleconnection patterns', *Int. J Climatol.*, **13**, 111–149.

Egido, A., Egido, M., Seco, J. and Garmendia, J. 1991. 'Quantitative relationships of mean seasonal precipitation in the Tagus river basin (Spain)', *Int. J. Climatol.*, **11**, 1–8.

Font Tullot, I. 1983. *Climatología de España y Portugal*, Instituto Nacional de Meteorología, 296.

Font Tullot, I. 1988. *Historia del clima de España*, I.N.M., Madrid.

Fraedrich, K. and Muller, K. 1992. 'Climate anomalies in Europe associated with ENSO extremes', *Int. J. Climatol.*, **12**, 25–31.

Hastenrath, S. and Greischar, L. 1995. 'Prediction of the summer rainfall over South Africa', *J. Climate*, **8**, 1511–1518.

Hogg, W.D. 1995. 'Cycles and trends in time series of Canadian extreme rainfall', *6th International Meeting on Statistical Climatology*, *University College*, *Galway*, pp. 257–278.

Huang, J., van den Dool, H.M. and Barnston, A.G. 1996. 'Long-lead seasonal temperature prediction using optimal climate normals', *J. Climate*, **9**, 809–817.

Hulme, M. 1995. 'Estimating global changes in precipitation', *Weather*, **50**, 34–42.

Hurrell, J.W. and van Loon, H. 1995. 'Decadal trends in the North Atlantic Oscillation and relationships to regional temperature and precipitation', *6th International Meeting on Statistical Climatology*, *University College*, *Galway*. pp. 185–188.

IMSL, 1991. *STAT/LIBRARY. FORTRAN subroutines for statistical analysis*, STLB-QRF-EN 109-20.

Kiladis, G.N. and Diaz, H.F. 1989. 'Global climatic anomalies associated with extremes in the Southern Oscillation', *J. Climate*, **2**, 1067–1090.

Krepper, C.M., Scian, B.V. and Pierini, J.O. 1989. 'Time and space variability of rainfall in central-east Argentina', *J. Climate*, **2**, 39–47.

Kulkarni, A. and von Storch, H. 1995. 'Monte Carlo experiments on the effect of serial correlation on the Mann–Kendall test of trend', *Meteorol. Z.*, **4**, 82–85.

Kutiel, H., Maheras, P. and Guika, S. 1996. 'Circulation and extreme rainfall conditions in the eastern Mediterranean during the last century', *Int. J. Climatol.*, **16**, 73–92.

Labitzke, K. and van Loon, H. 1995. 'Connection between the troposphere and stratosphere on a decadal scale', *Tellus*, **47A**, 275–286.

Lamb, P.J. and Pepler, R.A. 1987. 'North Atlantic Oscillation and an application', *Bull. Am. Meteorol. Soc.*, **68**, 1218–1225.

Leathers, D.J., Yarnal, B. and Palecki, M.A. 1991. 'The Pacific/North American teleconnection pattern and United States climate. Part I: regional temperature and precipitation associations', *J. Climate*, **4**, 517–528.

Mitchell, J.M., Dzerdzeevskii, B., Flohn, H., Hofmeyr, W.L., Lamb, H,H., Rao, K.N. and Wallén, C.C. 1966. *Climate Change*, World Meteorological Organization, Geneva. No. 195.TP.100.

North, G.R., Bell, T.L., Cahalan R.F. and Moeng, F.J. 1982. 'Sampling errors in the estimation of empirical orthogonal functions', *Mon. Wea. Rev.*, **110**, 699–706.

Peixoto, J.P. and Oort, A.H. 1992. *Physics of Climate*, AIP, pp. 412–433.

Peterson, T. and Easterling, D.R. 1994. 'Creation of homogeneous composite climatological reference series', *Int. J. Climatol.*, **14**, 671–679.

Preisendorfer, R. 1988. *Principal Component Analysis in Meteorology and Oceanography*, *Developments in Atmospheric Science*, Vol. 17. Elsevier, Amsterdam.

Rasmusson, E.M. and Arkin, P.A. 1993. 'A global view of large-scale precipitation variability', *J. Climate*, **6**, 149–522.

Richman, M.B. 1986. 'Rotation of principal components', *J. Climatol.*, **6**, 29–35.

Rodo, X., Baert, E. and Comin, F.A. 1997. 'Variations in seasonal rainfall in Southern Europe during the present century: relationships with the North Atlantic Oscillation and the El Niño–Southern Oscillation', *Climate Dyn.*, **13**, 275–284.

Rodriguez, C., Hernandez, A., Fidalgo, M.R. and Garmendia, J. 1992. 'Statistical method of precipitation prediction', *Atmos. Res.*, **28**, 299–309.

Ropelewski, C.F. and Halpert, M.S. 1987. 'Global and regional scale precipitation patterns associated with El Niño/Southern Oscillation', *Mon. Wea. Rev.*, **115**, 1606–1626.

Rowell, D.P., Folland, C.K., Maskell, K. and Ward, M.N. 1995. 'Variability of summer rainfall over tropical north Africa (1906–92): observations and modelling', *Q. J. R. Meteorol. Soc.*, **121**, 664–704.

Sneyers, R. 1990. *On the Statistical Analysis of Series of Observations*, W.M.O. Technical Note 143, 6–15.

Vautard, R., Yiou, P. and Ghil, M. 1992. 'Singular-spectrum analysis: a toolkit for short, noisy chaotic signals', *Physica*, **D 58**, 95–126.

© 1998 Royal Meteorological Society

Vinnikov, K.Ya., Groisman, P.Ya. and Lugina, K.M. 1990. 'Empirical data on contemporary global climate changes (temperature and precipitation)', *J. Climate*, **3**, 66–677.
von Storch, H. 1995. 'Spatial patterns: EOFs and CCA', in *Analysis of Climate Variability'*, Springer-Verlag, Berlin, pp. 227–257.
von Storch, H., Zorita, E. and Cubasch, U. 1993. 'Downscaling of global climate change estimates to regional scales: an application to Iberian rainfall in winter time', *J. Climate*, **6**, 1161–1171.
Wallace, J.M. and Gutzler, D.S. 1981.'Teleconnection in the geopotential height field during the Northern Hemisphere winter', *Mon. Wea. Rev.*, **109**, 784–812.
Wheeler, D. and Tout, D. 1990. 'The early autumn storms of 1989 in eastern Spain', *J. Meteorol.*, **15**, 238–248.
Wilks, D.S. 1996. 'Statistical significance of long-range optimal climate normal temperature and precipitation forecasts', *J. Climate*, **9**, 827–839.
Zorita, E., Hughes, J.P., Lettemaier, D.P. and von Storch, H. 1995. 'Stochastic characterization of regional circulation patterns for climate model diagnosis and estimation of local precipitation', *J. Climate*, **8**, 1023–1042.
Zorita, E., Kharin, V. and von Storch, H. 1992. 'The atmospheric circulation and sea surface temperature in the North Atlantic area in winter: their interaction and relevance for Iberian precipitation', *J. Climate*, **5**, 1097–1108.

© 1998 Royal Meteorological Society